Distibylation of Acetylenes with $Ph_2Sb–SbPh_2$: Synthesis, Crystal Structures and Phosphorescence Properties of Bis(diphenylstibyl)ethenes

Joji Ohshita[a], Toshiyuki Tsuchida[a], Kazuya Murakami[a], Yousuke Ooyama[a], Takayuki Nakanishi[b], Yasuchika Hasegawa[b], Norifumi Kobayashi[c], and Hideyuki Higashimura[c]

[a] Department of Applied Chemistry, Graduate School of Engineering, Hiroshima University, Higashi-Hiroshima 739-8527, Japan
[b] Division of Materials Chemistry, Graduate School of Engineering, Hokkaido University, Sapporo 060-8628, Japan
[c] Advanced Materials Research Labs, Sumitomo Chemical Co. Ltd., 6 Kitahara, Tsukuba 300-3294, Japan

Reprint requests to J. Ohshita. Fax: +81-82-424-5494. E-mail: jo@hiroshima-u.ac.jp

Z. Naturforsch. **2014**, *69b*, 1181 – 1187 / DOI: 10.5560/ZNB.2014-4166
Received July 31, 2014

Dedicated to Professor Hubert Schmidbaur on the occasion of his 80th birthday

Treatment of tetraphenyldistibine (**1**) with terminal arylacetylenes, $XC_6H_5C{\equiv}CH$ (**2a**–**c**, X = H, F, OMe), gave the corresponding *anti*-addition products (*E*)-aryl-1,2-bis(diphenylstibyl)ethenes **3a**–**c** in 11 – 17 % yields. A similar reaction of **1** with 1,4-diphenylbutadiyne provided (*E*)-1,4-diphenyl-1,2-bis(diphenylstibyl)but-1-en-3-yne (**3d**) in 28 % yield. X-Ray diffraction studies on crystals of **3a**, **3b** and **3d** revealed a congested configuration around the ethylene core. The optical properties of the adducts **3a-d** were examined by measuring UV absorption and photoluminescence spectra. Interestingly, **3d** showed phosphorescence in the solid state, which was enhanced at low temperature.

Key words: Distibine, Distibylethene, Phosphorescence, Crystal Structure

Introduction

Organic Sb–Sb bonds are usually highly reactive and readily undergo atmospheric oxidation unless sterically bulky groups, such as *t*-Bu, CH_2SiMe_3, Ph, and Mes, are present at the Sb atoms for kinetic stabilization [1 – 3]. The insertion of low-valent transition metal compounds into Sb–Sb bonds [4, 5] and the homolytic cleavage leading to stibyl radicals in the presence of organic radical initiators [6] have been reported. However, only a limited number of chemical reactions involving Sb–Sb bonds are known. Naka and coworkers reported an interesting polymerization of pentaphenylcyclopentastibine $(PhSb)_5$ with dimethyl acetylenedicarboxylate $MeO_2CC{\equiv}CCO_2Me$ induced by AIBN [7]. The polymerization proceeded smoothly *via* a radical process to provide a polymer consisting of alternating dimethyl ethenylenedicarboxylate and phenylstibylene units (Scheme 1), as the sole example of the distibylation of unsaturated carbon-carbon bonds. To date, there is no example for the simple addition reaction of organodistibine to unsaturated carbon-carbon bonds, despite the fact that a similar diphosphination reaction of acetylene with diphosphines has been studied under several conditions as a direct route to diphosphanyl compounds, which may be used as bidentate ligands [8 – 10]. The diarsination reaction of acetylene is also rare [7].

In this paper, we report for the first time the distibylation of unsaturated carbon-carbon bonds with distibine. Terminal arylacetylenes and diphenylbutadiyne react readily with tetraphenyldistibine to give *anti*-adducts. This reaction offers a single-step route to (*E*)-bis(diphenylstibyl)ethenes. Although some *o*-distibylbenzenes have been prepared [11 – 16], they require multiple steps for synthesis, and no practical method leading to linear bis(diphenylstibyl)ethenes has been demonstrated [11]. The crystal structures of three bis(diphenylstibyl)ethenes were determined by X-ray diffraction analyses. Their optical proper-

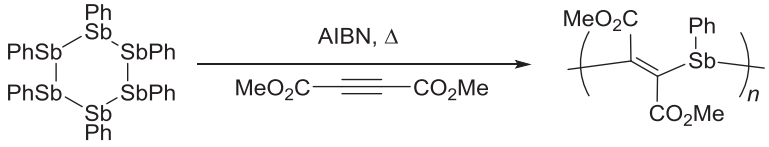

Scheme 1. Formation of a stibylene-ethenylene polymer [7].

ties were also investigated, and solid-state phosphorescence was noted for the adduct derived from 1,4-diphenylbutadiyne.

Results and Discussion

*Reactions of tetraphenyldistibine (**1**) with acetylenes*

Treatment of tetraphenyldistibine (**1**) with 10 equiv. of phenylacetylene (**2a**) at 60°C for 2 h, followed by recrystallization of the product from toluene afforded 1 : 1 the *anti*-adduct (*E*)-1,2-bis(diphenylstibyl)phenylethene (**3a**) in 15% isolated yield, as shown in Scheme 2. Carrying out the reaction with 1 equiv. of **2a** in toluene did not alter the results. The low yield was due to the difficult purification **3a**, and direct NMR analysis of the reaction mixture revealed no signals ascribable to other major products. Indeed, the yield of **3a** as estimated from the ^{1}H NMR spectrum of the reaction mixture using mesitylene as the internal standard was approximately 70%. No *Z*-isomer was formed in this reaction. Distibine **1** also reacted with *p*-fluoro- and *p*-methoxyphenylacetylene (**2b** and **2c**) to give selectively the *anti*-adducts **3b** and **3c**, respectively.

Similar reactions of **1** with 1- and 4-octyne, diphenylacetylene, dimethyl acetylenedicarbonate (DMAC), and (trimethylsilyl)acetylene did not proceed at all even at 100°C, and the reactants were recovered unchanged. Distibine **1** did also not react with styrene or 2,3-dimethylbutadiene. In contrast, **1** reacted smoothly with 1,4-diphenylbutadiene (**2d**) to give adduct **3d** in 28% isolated yield, which was higher than those of **3a–c**, presumably reflecting the higher crystallinity of **3d**. Compounds **3a–d** are stable in air as solids, but undergo air oxidation slowly in solution to give complex mixtures, including an insoluble colorless powder. The chemical structures were verified by MS and NMR spectroscopy, and the (*E*)-configuration was confirmed by single-crystal X-ray diffraction studies (*vide infra*). The reaction mechanism of the present distibylation remains unclear. However, the fact that the addition reactions proceeded smoothly regardless of the substituent on the phenyl ring (X) and the inertness of the inner acetylenes and the terminal alkyl- and silylacety-

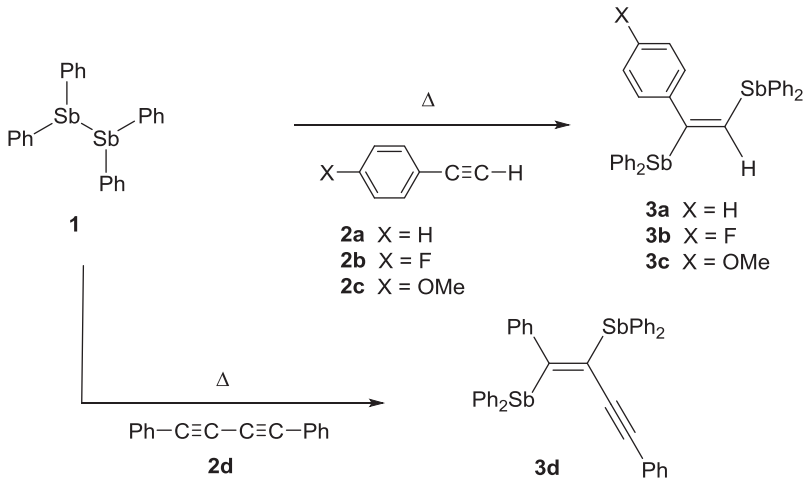

Scheme 2. Addition of tetraphenyldistibine to arylacetylenes.

lene towards the addition of **1**, seems to indicate that a radical process, including the formation of a diphenylstibyl radical, is involved in the reactions. This contrasts a similar diphosphination of acetylenes with diphosphine, which requires UV irradiation or radical initiators to promote the reaction. One exception is the addition of diphosphines to DMAC. In that reaction, the nucleophilic addition of diphosphines occurs at the acetylene carbon to give zwitterionic intermediates that are stabilized by delocalization of the anionic charge over the ester unit, from which migration of the diphenylphosphinyl group takes place to give the *syn*-adducts, (*Z*)-isomers [8]. In the present case, however, distibine **1** did not react with DMAC, and only (*E*)-isomers were obtained from **2a**–**d** with complete stereoselectivity, thereby excluding the possibility of the nucleophilic addition mechanism.

*Crystal and molecular structures of the bis(diphenylstibyl)ethenes **3a**, **3b** and **3d***

Compounds **3a**, **3b** and **3d** were recrystallized from toluene to afford single crystals suitable for X-ray diffraction studies. In Fig. 1, showing the ORTEP drawings of the compounds, the congested configurations around the ethylene cores become obvious. Selected bond lengths, angles, and torsion angles are listed in Table 1. The twisting of the ethylene units is likely

Table 1. Selected bond lengths (Å), angles (deg), and torsion angles (deg) for **3a**, **3b** and **3d** with estimated standard deviations in parentheses.

	3a	**3b**	**3d**
Distances			
Sb1–C1	2.167(5)	2.181(4)	2.180(3)
Sb2–C2	2.185(5)	2.144(4)	2.188(3)
C1–C2	1.321(8)	1.327(6)	1.355(5)
Angles			
Sb1–C1–C2	119.7(4)	117.5(3)	118.2(3)
Sb1–C1–Ph	115.9(4)	117. 9(3)	117.2(2)
Ph–C1–C2	124.2(5)	124.6(3)	124.3(3)
Sb2–C2–C3			119.8(3)
Sb2–C2–C1	128.9(4)	128.9(3)	119.2(3)
C1–C2–C3			120.7(3)
Ph–Sb1–Ph	96.0(2)	98.9(2)	96.2(1)
C1–Sb1–Ph	94.7(2), 98.7(2)	92.3(2), 98.5(2)	96.6(1), 99.5(1)
Ph–Sb2–Ph	94.0(2)	93. 9(2)	97.7(1)
C2–Sb2–Ph	88.6(2), 95.2(2)	89.6(1), 96.5(2)	95.7(1), 100.4(1)
Torsion angles			
Sb1–C1–C2–Sb2	178. 8(3)	167.1(3)	177.8(1)

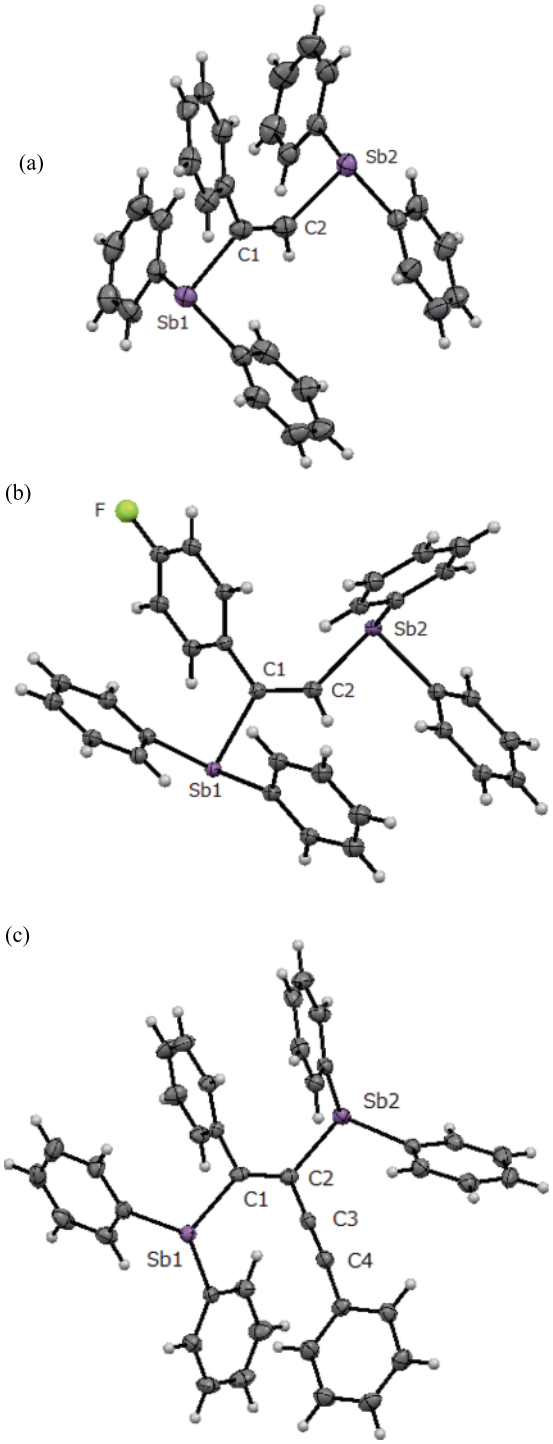

Fig. 1 (color online). ORTEP drawings of **3a**, **3b** and **3d** (from top to bottom). Displacement ellipsoids are drawn at the 50 % probability level.

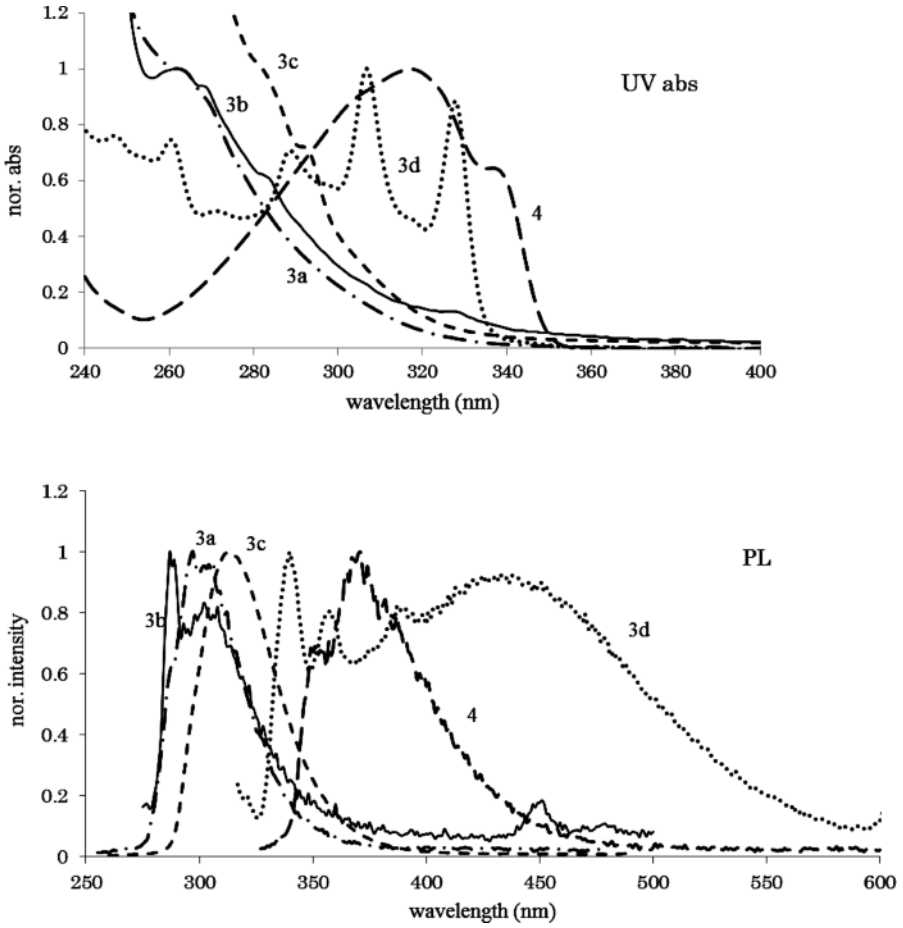

Fig. 2. UV absorption (top) and photoluminescence (bottom) spectra of **3a**–**d** in THF.

due to the steric repulsion between the bulky substituents. The smallest torsion angle of Sb1–C1–C2–Sb2 = 167.1(3)° is seen in **3b**. The large angles of Ph–C1–C2 in **3a**, **3b** and **3d** and of C1–C2–Sb2 in **3a** and **3b** are also indicative of the steric repulsion between phenyl and diphenylstibyl units located in a *cis* fashion. The ethylene C=C distances in **3a** and **3b** are within the standard range (average distance for trisubstituted ethenes: 1.326 Å, aryl ethenes: 1.339 Å) [15]. The structure parameters involving the Sb atoms are also in the normal range with slight deviations from the standard angles of *p*-bonded substituents, again reflecting the steric repulsion between the substituents. In fact, it has been reported that the less congested $Ph_2SbOSbPh_2$ exhibits less deviating Ph–Sb–Ph angles of 93.8° and 94.9° [2]. The Ph–Sb distances of **3a**, **3b** and **3d** are in the range between 2.143 and 2.169 Å, and are comparable to those of $Ph_2SbOSbPh_2$ (2.143 – 2.156 Å). There are no important intermolecular contacts in the crystal.

*Optical properties of the bis(diphenylstibyl)ethenes **3a**–**3d***

The optical properties of the bis(diphenylstibyl)-ethenes **3a**–**d** were examined by measuring the UV absorption and photoluminescence (PL) spectra. Fig. 2 presents the spectra measured in THF at room temperature. The UV spectra of **3a**–**c** show shoulders around 260 – 290 nm, together with the major absorption bands at approximately 250 nm. The wavelengths of the major absorption bands are similar to that of Ph_3Sb (λ_{max} = 258 nm in THF), and they are ascribed to the diphenylstibyl units. On the other hand,

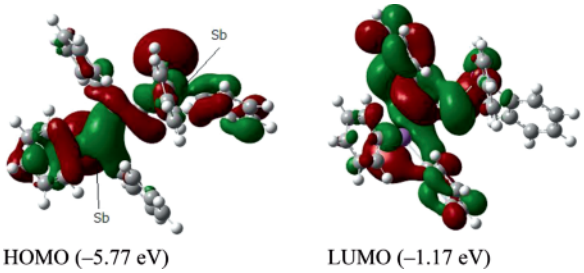

Fig. 3 (color online). HOMO and LUMO profiles and energy levels of **3a**, derived from DFT calculations at the B3LYP/LANL2DZ level of theory.

the shoulders at longer wavelengths seem to be due to the bis(diphenylstibyl)ethylene cores. Fig. 3 shows the HOMO and LUMO profiles of **3a**, which are derived from quantum-chemical calculations at the B3LYP/LANL2DZ level of theory. The profiles indicate the contribution of the Sb orbital to both HOMO and LUMO. The phenyl ring on carbon is nearly perpendicular to the ethylene core unit and has little orbital interaction in the HOMO, and the phenyl orbital is to some extent only involved in the LUMO.

The absorption bands of **3d** appear at lower energies than those of **3a–c**, reflecting the longer conjugation of the diphenylbutenyne system. To understand the influence of the stibyl substitution in **3d**, we prepared 1,4-diphenylbut-1-en-3-yne (**4**). In contrast to **3d** which shows rather sharp absorption bands, a broad absorption band centered at $\lambda_{max} = 318$ nm is observed for **4**, accompanied by a small shoulder at approximately 337 nm. Although the reason for the sharp bands of **3d** is not yet clearly understood, it can be said that the bulky diphenylstibyl substituents restrict the molecular vibration and are therefore partly responsible for the spectral shape. Fig. 4 shows the HOMO and LUMO profiles of **3d** and **4**, derived from DFT calculations. Both HOMO and LUMO of **4** are well delocalized over the diphenylbutenyne unit. In contrast, the phenyl *p*-orbital on the ethylene carbon of **3d** is involved in the HOMO to a certain extent, whereas its contribution to the LUMO is rather limited, similar to those of **3a** (Fig. 3). Although orbital interaction between the diphenylstibyl substituents and the diphenylbutenyne core is clearly seen in the HOMO and LUMO profiles of **3d**, a twist of the Ph–C=C unit would lead to a larger HOMO-LUMO gap for **3d** than for **4**.

As shown in Fig. 2 the present bis(diphenylstibyl)-ethenes exhibit photoluminescence (PL), although the

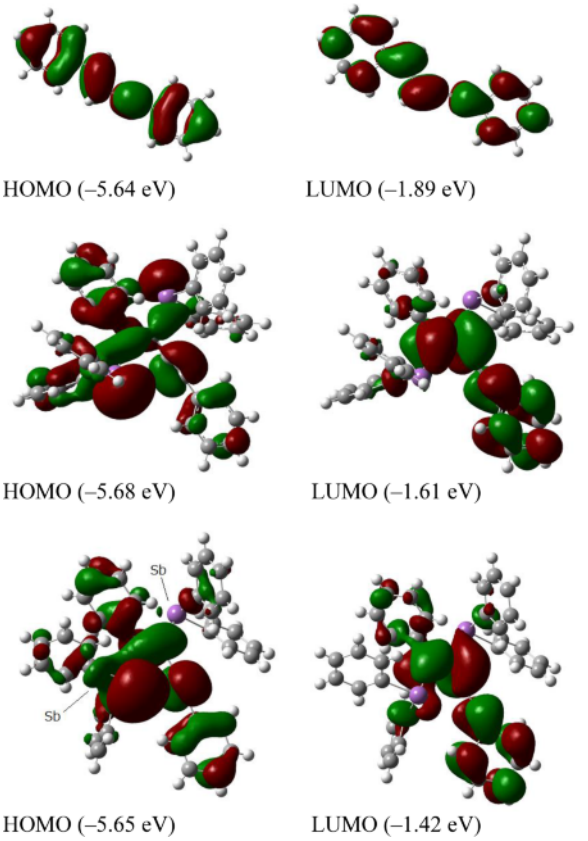

Fig. 4 (color online). HOMO and LUMO profiles and energy levels of **4** (top) and **3d** optimized in the gas phase (middle), and **3d** with the geometry determined by X-ray diffraction (bottom), derived from DFT calculations at B3LYP/LANL2DZ level of theory.

PL quantum yields are low ($\Phi < 2\,\%$). The PL spectrum of compound **3d** shows a broad band centered at approximately $\lambda_{max} = 430$ nm, its wavelength being longer than those of **3a–c** ($\lambda_{max} = 300 - 320$ nm) and **4** ($\lambda_{max} = 370$ nm). Interestingly, the PL band of **3d** is even more red-shifted when measurements are carried out on solid **3d**. Since no important intermolecular interactions are observed in the crystal structure of **3d**, the reason for the redshift is not yet known. It is possible that there is a higher degree of conjugation in the crystal than in solution. However, single-point energy calculations of the crystal structure of **3d** reveal a larger HOMO-LUMO energy gap (4.24 eV) than that of the fully optimized structure in the gas phase (4.08 eV, see Fig. 4).

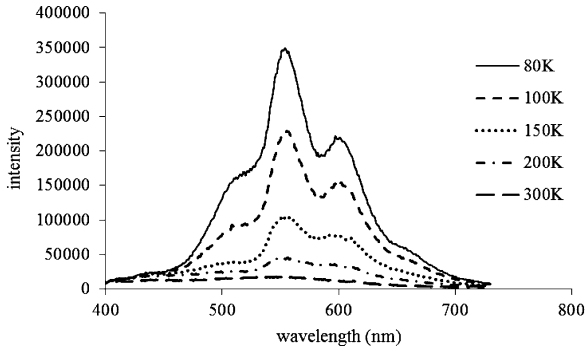

Fig. 5. Temperature-dependent emission spectra of **3d** in the solid state.

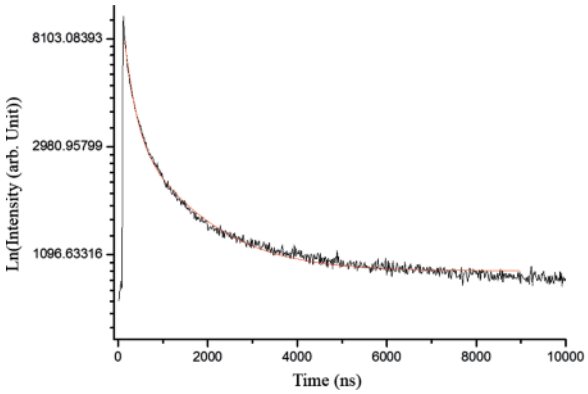

Fig. 6 (color online). PL decay plot of **3d** in the solid state at 80 K, excited at 375 nm, and a fitting curve with the two components $\tau_1 = 0.18\,\mu$s (30%) and $\tau_2 = 1.0\,\mu$s (70%).

Interestingly, as presented in Fig. 5, the solid-state PL band of **3d** is markedly intensified as the temperature is lowered, and that characteristic is common to phosphorescence bands. As shown in Fig. 6, the PL decay plot obtained at 80 K fits well the two-component curve with $\tau_1 = 0.18\,\mu$s (30%) and $\tau_2 = 1.0\,\mu$s (70%). Although solid-state PL is usually complicated because of energy migration, the data clearly indicate that the PL band is ascribed to phosphorescence.

In conclusion, we have demonstrated that the addition of distibine to terminal arylacetylene or diphenyldiyne proceeded smoothly in an *anti* fashion to provide (*E*)-bisstibylethenes. (*E*)-Bisstibylbutenyne **3d** showed phosphorescence in the solid state. The Sb heavy-atom effects and the highly rigid structure arising from the congested environment around the diphenylbutenyne chromophore seem to be responsible for the phosphorescence.

Experimental Section

All reactions were carried out in dry argon. Distibine **1** [6] and 1,4-diphenylbut-1-en-3-yne [18] were prepared as reported in the literature. NMR spectra were recorded on a Varian 400-MR spectrometer. High-resolution APCI mass spectra were measured on a Thermo Fisher Scientific LTQ Orbitrap XL spectrometer at N-BARD, Hiroshima University. Room-temperature UV/Vis absorption and PL spectra were measured on Hitachi U-3210 and Horiba FluoroMax-4 spectrophotometers, respectively. Measurements at low temperature (77 – 300 K) were performed with a nitrogen cryostat (Oxford Instruments, Optistat DN) and a temperature controller (Oxford Instruments, ITC 502S), or with a CoolSpeK UV temperature controller (Unisoku Co. Ltd., USP-203-A). Emission life times were measured on a Spec Fluorolog-3ps instrument with a lightsource of nanoLED 370 nm (pulse width = 1.5 ns).

*(E)-1-Aryl-1,2-bis(diphenylstibyl)ethenes **3a–3d***

To a 5 mL Schlenk tube was introduced a mixture of 1.10 g (2.00 mmol) of tetraphenyldistibine (**1**) and 2 mL (10 eq.) of phenylacetylene (**2a**). The mixture was stirred at 60°C for 10 h. Excess **2a** was evaporated under reduced pressure, and the residue was recrystallized from toluene to give 0.22 g (15% yield) of adduct **3a**. M. p.: 86.2–87.4°C. – ^{1}H NMR (400 MHz, $CDCl_3$): δ = 7.04 (dd, 2H, J = 7.6, 2.0 Hz, *o*-Ph), 7.16 – 7.18 (m, 2H, Ph), 7.20 (s, 1H, HC=), 7.22 – 7.31 (m, 13H, Ph), 7.34 (dd, 4H, J = 7.6, 1.6 Hz, *o*-Ph), 7.43 ppm (dd, 4H, J = 7.6, 1.6 Hz, *o*-Ph). – ^{13}C NMR ($CDCl_3$): δ = 127.02, 127.49, 128.18, 128.22, 128.61, 128.85, 135.65, 136.14, 139.68, 139.74 (Ph), 144.95 (C(H)(Sb)=), 145.25 (C(Ph)(Sb)=), 160.41 ppm (*i*-C of Ph–C=). – HRMS (APCI): m/z = 653.01836 (calcd. 653.01887 for $C_{32}H_{26}Sb_2$, $[M+H]^+$).

The other distibylethylenes **3b–3d** were prepared in a similar manner.

*Data for **3b***: M. p. 126.3–127.4°C. – ^{1}H NMR (400 MHz, $CDCl_3$): δ = 6.81 – 6.86 (m, 2H, C_6H_4F), 6.91 – 6.95 (m, 2H, C_6H_4F), 7.21 (s, 1H, HC=), 7.24 – 7.32 (m, 12H, Ph), 7.34 (dd, 4H, J = 7.2, 2.0 Hz, *o*-Ph), 7.41 ppm (dd, 4H, J = 7.6, 2.0 Hz, *o*-Ph). – ^{13}C NMR ($CDCl_3$): δ = 115.07 (d, m-(C_6H_4F)–C=, J = 22 Hz), 128.28, 128.66, 128.70, 128.90 (Ph), 129.04 (d, *o*-C, Ph-C=, J = 8 Hz), 135.66, 136.09 (*o*-C, Ph-Sb), 139.45, 139.47 (*i*-C, Ph-Sb), 141.24 (d, *i*-C of (C_6H_4F)-C=, J = 3 Hz), 145.65 (C(H)(Sb)=), 159.43 (C(C_6H_4F)(Sb)=), 160.83 ppm (d, *p*-C of (C_6H_4F)-C=, J = 253 Hz). HRMS (APCI): m/z = 671.00942 (calcd. 671.00894 for $C_{32}H_{25}FSb_2$, $[M+H]^+$).

*Data for **3c***: M. p. 102.4–103.8°C. – ^{1}H NMR (400 MHz, $CDCl_3$): δ = 3.76 (s, 3H, MeO-), 6.72 (d, 2H, J = 8.8 Hz, C_6H_4OMe), 6.99 (d, 2H, J = 8.4 Hz, C_6H_4OMe), 7.12 (s, 1H, HC=), 7.20 – 7.31 (m, 12H, Ph), 7.33 (dd, 4H, J =

7.4, 1.8 Hz, *o*-Ph), 7.43 ppm (dd, 4H, J = 7.4, 1.8 Hz, *o*-Ph). – ^{13}C NMR ($CDCl_3$): δ = 55.21 (MeO), 113.59 (*m*-C, Ph-Sb), 128.15, 128.56, 128.59, 128.79, 128.84 (Ph and C_6H_4OMe), 135.64, 136.16 (*o*-C, Ph-Sb), 137.85 (*i*-C of (C_6H_4OMe)-C=), 139.73, 139.84 (*o*-C of Ph-Sb), 144.21 (C(H)(Sb)=), 158.720 (*p*-C of (C_6H_4OMe)-C=), 159.96 ppm (C(C_6H_4OMe)(Sb)=). – HRMS (APCI): m/z = 683.02923 (calcd. 683.02893 for $C_{33}H_{29}OSb_2$, $[M+H]^+$).

Data for ***3d***: M. p. 114.8–116.0°C. – ^{1}H NMR (400 MHz, $CDCl_3$): δ = 6.58 (dd, 2H, J = 8.2, 1.4 Hz, *o*-Ph), 6.73 (dd, 2H, J = 8.2, 1.4 Hz, *o*-Ph), 6.90 – 6.99 (m, 3H, Ph) 7.10 – 7.23 (m, 9H), 7.31 – 7.36 (m, 10H), 7.55 – 7.58 ppm (m, 4H, *o*-Ph). – ^{13}C NMR ($CDCl_3$): δ = 91.79, 101.01 (C≡C), 123.04 (*i*-C of Ph-C≡), 126.50, 127.38, 127.74, 127.86, 128.01, 128.12, 128.38, 128.43, 128.65, 131.26 (Ph), 136.09, 136.37 (*o*-C of Ph-Sb), 139.74 (2C, *o*-C of Ph-Sb), 140.76 (C(C≡C)(Sb)=), 143.47 (*i*-C of Ph-C=), 168.13 ppm (C(Ph)(Sb)=). – HRMS (APCI): m/z = 753.05085 (calcd. 753.04966 for $C_{40}H_{30}Sb_2$, $[M+H]^+$).

Crystal structure determinations

Single crystals of **3a**, **3b** and **3d** suitable for X-ray diffraction studies were obtained by repeated recrystallization from toluene. Data were collected at −150°C on a Rigaku R-AXIS RAPD diffractometer using graphite-monochromatized MoK_α radiation. The structures were solved by a Direct Methods (SHELXS-97 [17, 18]) and expanded using Fourier techniques. Non-hydrogen atoms were refined anisotropically, whereas hydrogen atoms were included but not refined (SHELXL-97 [17, 18]). All other calculations were performed using the CRYSTALSTRUCTURE crystallographic software package of Rigaku Corporation.

CCDC 1014264 – 1014266 contain the supplementary crystallographic data for this paper. These data can be obtained free of charge from The Cambridge Crystallographic Data Centre *via* www.ccdc.cam.ac.uk/data_request/cif.

Acknowledgement

This work was supported by a Grant-in-Aid for Scientific Research on Innovative Areas "New Polymeric Materials Based on Element-Blocks (no. 2401)" of The Ministry of Education, Culture, Sports, Science, and Technology, Japan. We also thank Dr. Hiroshi Fukuoka, Hiroshima University, for assistance in X-ray diffraction studies.

[1] J. L. Wardell in *Comprehensive Organometallic Chemistry II*, Vol. 2 (Eds.: E. W. Abel, F. G. A. Stone, G. Wilkinson), Elsevior, Oxford, **1995**, chapter 8, p. 321.
[2] H. J. Breunig, T. Krüger, E. Lork, *J. Organomet. Chem.* **2002**, *648*, 209 – 213.
[3] H. J. Breunig, R. Rösler, *Chem. Soc. Rev.* **2000**, *29*, 403 – 410.
[4] Y.-Z. Li, R. Ganguly, W. K. Leong, *Organometallics* **2014**, *33*, 823 – 828.
[5] H. J. Breunig, I. Ghesner, M. E. Ghesner, E. Lork, *J. Organomet. Chem.* **2003**, *677*, 15 – 20.
[6] E. Kayahara, N. Kondo, S. Yamago, *Heteroatom Chem.* **2011**, *22*, 307 – 31.
[7] K. Naka, *Polymer Journal* **2008**, *40*, 1031 – 1041.
[8] A. Sato, H. Yorimitsu, K. Oshima, *Angew. Chem. Int. Ed.* **2005**, *44*, 1694 – 1696.
[9] S. Kawaguchi, S. Nagata, T. Shirai, K. Tsuchii, A. Nomoto, A. Ogawa, *Tetrahedron Lett.* **2006**, *47*, 3919 – 3922.
[10] D. L. Dodds, M. F. Haddow, A. G. Orpen, P. G. Pringle, G. Woodward, *Organometallics* **2006**, *25*, 5937 – 5945.
[11] W. Levason, C. A. McAuliffe, S. G. Murray, *J. Organomet. Chem.* **1975**, *88*, 171 – 174.
[12] R. E. Humphries, N. A. A. Al-Jabar, D. Bowen, A. G. Massey, G. B. Deacon, *J. Organomet. Chem.* **1987**, *319*, 59 – 67.
[13] Y. Uchiyama, J. Sugimoto, M. Shibata, G. Yamamoto, Y. Mazaki, *Bull. Chem. Soc. Jpn.* **2009**, *82*, 819 – 828.
[14] Y. Uchiyama, *Heteroatom Chem.* **2011**, *22*, 377 – 387.
[15] D. R. Lide (Ed.), *Handbook of Chemistry and Physics*, 76th edition, CRS Press, New York, **1995**.
[16] K. Okuro, M. Furuune, M. Enna, M. Miura, M. Nomura, *J. Org. Chem.* **1993**, *58*, 4716 – 4721.
[17] G. M. Sheldrick, SHELXS/L-97, Programs for Crystal Structure Determination, University of Göttingen, Göttingen (Germany) **1997**.
[18] G. M. Sheldrick, *Acta Crystallogr.* **2008**, *A64*, 112 – 122.